

NACA TN 3510

# NATIONAL ADVISORY COMMITTEE FOR AERONAUTICS

TECHNICAL NOTE 3510

AN AUTOMATIC VISCOMETER FOR NON-NEWTONIAN MATERIALS

By Ruth N. Weltmann and Perry W. Kuhns

Lewis Flight Propulsion Laboratory  
Cleveland, Ohio



Washington  
August 1955

NATIONAL ADVISORY COMMITTEE FOR AERONAUTICS

TECHNICAL NOTE 3510

AN AUTOMATIC VISCOMETER FOR NON-NEWTONIAN MATERIALS

By Ruth N. Weltmann and Perry W. Kuhns

SUMMARY

A concentric-cylinder rotational viscometer is described that is capable of recording meaningful flow curves of rate of shear against shearing stress for most non-Newtonian materials. For many of these materials the flow curve depends on the flow condition of measurement, that is, on the rate of change and the magnitude of the applied flow parameter, which is the rate of shear in this viscometer. Therefore, this instrument incorporates features that permit the operator to program the flow conditions, which are used to produce the flow curve. The instrument is designed so that for most materials the rate of shear is proportional to the rotational speed. A program feature permits presetting the maximum rotational speed to any speed from 80 to 1600 rpm. The speed is automatically varied. The acceleration is constant and can be selected, so that 15, 30, 60, 120, or 240 seconds are required for the speed to change from zero to the preset maximum. Ranges of increasing and decreasing speeds can be programmed to follow each other in two different sequences. The viscometer can also record shearing-stress changes as a function of time at given constant rates of shear.

Rates of shear up to 4000 seconds<sup>-1</sup> can be obtained under laminar flow conditions. The instrument is built to measure shearing stresses from 50 to 250,000 dynes/cm<sup>2</sup>. Viscosities up to 3000 poises can be measured automatically, and up to 20,000 poises manually. Friction is kept at a minimum to permit viscosity measurements down to 0.05 poise.

The coaxial alinement of the two cylinders is mechanically fixed. The annuli between the cylindrical surfaces are designed to give (1) maximum shearing stresses for any given motor torque, (2) less than 15-percent variation in shearing stress across their width, and (3) minimum increase in shear temperature during operation. End effects are minimized by the design so that they can be neglected. Accessories are incorporated to keep the shear volume of the material constant and confined. A constant-temperature bath is provided. The instrument can be readily modified for dynamic flow measurements up to frequencies of 4 cps. Flow curves, time-torque curves, and dynamic viscosity data are presented to demonstrate the versatility of the viscometer.

3698

CB-1

## INTRODUCTION

The transfer behavior of fuels and lubricants, when they are passed through an aircraft propulsion system, is greatly controlled by the flow properties of these fluids. Most of these fluids are of Newtonian character, but some have non-Newtonian and frequently also time-dependent flow properties under the required operational conditions of temperature and stress. Thus, an instrument was designed to measure the non-Newtonian flow parameters of such aircraft fluids.

The apparent viscosity of a material is commonly defined as the ratio of shearing stress to rate of shear. For a Newtonian fluid this ratio remains constant under all flow conditions. Thus, for a Newtonian material the apparent viscosity is the Newtonian viscosity, which can be determined at any one flow condition. For many non-Newtonian materials, however, the apparent viscosity varies with the flow conditions of measurement, that is, with the rate of change and magnitude of the rate of shear or shearing stress. Therefore, measurements at at least two well-defined flow conditions are necessary, and in many cases an extended range of measurements is required, before a valid interpretation of the flow behavior of a non-Newtonian material is possible. For this reason a viscometer for a meaningful measurement of the flow properties of non-Newtonian materials must be capable of producing curves of rate of shear  $G$  against shearing stress  $\tau$  over an extended range of flow conditions, and in accordance with a controlled program. The choice of the program depends on the required information and the nature of the test material. Such programmed curves of rate of shear against shearing stress are termed "flow curves." For convenience, it is desirable that the viscometer incorporate means of recording these flow curves. Since the flow properties of most materials change with temperature, a flow curve has meaning only if it is produced under constant-temperature conditions. Thus, the viscometer must have the following characteristics:

(1) It must be possible to apply an increasing and decreasing rate of shear at given constant rates of change and over different and extensive ranges of rate of shear to the same sample of material.

(2) The rate of shear must at any one instant be independent of the mechanical loading, and its value must be measurable and reproducible. At the same time the stress produced in the sample by the instantaneous applied rate of shear must be measurable and reproducible.

(3) The geometrical confines of the sheared sample must be simple and remain unchanged by the applied forces, and the flow must be laminar up to the highest rates of shear, so that a mathematical analysis can be made based on a known model of flow.

(4) End effects should be minimized, since they cannot be evaluated mathematically.

(5) The rate of shear and shearing stress within the sheared sample should be as uniform as feasible. This is necessary since  $G$  and  $\tau$

are not measured directly but are derived from velocity and force. For non-Newtonian materials, the flow resistance changes with  $G/\tau$  and thus will vary within the sheared sample if  $G$  and  $\tau$  vary. Then, the recorded curve is no longer a  $G$  against  $\tau$  curve unless the knowledge of the force and velocity distributions within the sheared sample permit an exact mathematical analysis to obtain  $G$  as a function of velocity and  $\tau$  as a function of force.

(6) Temperature increases due to shear should be kept at a minimum by proper design and by temperature control.

For information on the time-dependence of the flow properties of some materials, it is important that such a viscometer be capable of recording curves of shearing stress as a function of time, when subjected to constant rates of shear.

Only some viscometers described in the literature (refs. 1 to 9) are suitable for high rate of shear applications and incorporate some of the abovementioned features. This paper describes a concentric-cylinder rotational viscometer, developed at the NACA Lewis laboratory, which combines all the previously listed features. The viscometer can be used over a wide range of rates of shear up to  $4000 \text{ sec}^{-1}$ . The rate of shear can be varied automatically at a constant preselected acceleration and in two predetermined sequences. With this viscometer meaningful flow curves can be produced for materials varying greatly in the degree of non-Newtonian behavior and in flow resistance. Viscosities can be measured ranging from 0.05 to 20,000 poises. The sample is confined in annuli between two cylinders that are mechanically fixed in a coaxial position. The annuli are designed to make end effects negligible and to minimize temperature effects and variations in shearing forces across their width. The flow remains laminar under all flow conditions. The versatility of this instrument is demonstrated by a few flow-curve measurements and some other data.

#### SYMBOLS

The following symbols are used in this report:

$f$	Bingham yield value, $[\text{ML}^{-1}\text{T}^{-2}]$
$G$	rate of shear, $[\text{T}^{-1}]$
$K_G$	defined by eq. (2)
$K_\tau$	defined by eq. (3)
$L$	length of annulus between cup and bob, $[\text{L}]$
$n$	rotational speed in revolutions per unit time, $[\text{T}^{-1}]$
$R_i$	radius of inner cylinder (bob), $[\text{L}]$

$R_c$	radius of outer cylinder (cup), [L]
$Re$	Reynolds number, $2\pi n R_c^2 \left(1 - \frac{R_b}{R_c}\right) \rho / \mu$
$T$	torque, $[ML^2T^{-2}]$
$t$	time, [T]
$U$	plastic viscosity, $[ML^{-1}T^{-1}]$
$\eta$	apparent viscosity, $[ML^{-1}T^{-1}]$
$\theta$	timing of flow curve from zero to preset maximum, [T]
$\mu$	Newtonian viscosity, $[ML^{-1}T^{-1}]$
$\rho$	density, $[ML^{-3}]$
$\tau$	shearing stress, $[ML^{-1}T^{-2}]$

## Subscripts:

cr	critical
int	intercept
max	maximum

## CONSTRUCTION

The viscometer is shown in figures 1 to 3. The sample is sheared between the two coaxial cylindrical surfaces (fig. 3). The outer cylinder, which is designated the cup, is rotated by a servo-type motor. The motor is geared to a tachometer, the output of which is proportional to the rotational speed of the cup. The torque on the stationary cylinder, designated the bob, is measured with a transducer which is a strain-gage assembly. The output of the tachometer is fed into one side, and the output of the transducer into the other side of an x-y recorder. The rate of shear is, for most materials, proportional to the rotational speed, and the shearing stress is proportional to the torque. Thus, for most materials, the recorded curve is a curve of rate of shear as a function of shearing stress.

One side of the recorder, instead of being connected to the tachometer output, may be moved at a constant speed. Then one axis of the

paper becomes a time axis, while the other axis measures the output from the strain gage. Thus, curves of shearing stress as a function of time are recorded.

### Cylinder Assembly

Figures 2 and 3 show some parts of the viscometer in detail. Figure 2 is a photograph and figure 3 is a diagram of the cylinder assembly and some associated parts. The cylinder assembly is mounted on a stand (fig. 1) and can be moved up and down by turning a hand wheel. The cup and bob (fig. 3) are mounted each in two sets of ball bearings. The one-piece bearing holder keeps both cylinders permanently coaxially aligned with respect to each other.

The cup is removable for filling and cleaning purposes. Accidental damage to the bob, such as bending, can occur when the cup is removed by hand. To prevent this, a tool is affixed to the base of the stand. This cup tool can be rotated in and out of position. The cup is first loosened by unscrewing the cup ring. Then the cylinder assembly is moved down until the bottom of the cup touches the base of the stand. The cup tool is rotated into position and thus engages the cup above its bottom part. In this position the axis of the cup tool and the cup axis coincide. As the assembly is moved up, the cup is left behind in the cup tool. To attach a filled cup to the assembly, the reverse procedure is followed. A conical shoulder is provided to engage the cup ring to the cup. The upper part of the cup (fig. 2) fits over the mounting assembly. It is slotted, so that its upper diameter is contracted to fit tightly around the mounting cylinder when the cup ring is screwed on and the cup is pulled up. In this way concentricity is repeatedly achieved. To keep the cup axis parallel with the bob axis, the cup is pulled up against a flat shoulder.

The diameters of the bob shaft and of its bearings are kept very small, to minimize friction. The bob is held in the assembly by a collar that rests on the upper surface of the upper bearing, which is a combination radial-thrust bearing.

In addition to the coaxial alinement of the cup and bob, which is mechanically fixed, the cylinder axes have to be maintained parallel and straight. The parallel alinement and straightness of both cylinder axes are checked with an indicator (fig. 2). Provision is made for mounting the indicator with respect to the cup axis and the assembly axis. This is very important, since even a slight parallel misalignment or bend in either axis can affect the measurement and lead to large errors in interpretation of the flow curve, as will be shown later.

### Cylinder Design

The three cylinder sets, consisting of three cups and two bobs, are designed to permit measurements over a wide range of viscosities and rates of shear, while maintaining the shearing stress across the annuli as nearly uniform as feasible. Thus, measurements on non-Newtonian materials are meaningful.

Since the distribution of the shearing stress within the material varies inversely with the square of the radius, the clearance between cup and bob is kept as small as is mechanically practicable. A small clearance is also desirable for better heat dissipation, so that the temperature increase produced in the material during shear is kept at a minimum (ref. 10).

The dimensions of the three cylinder sets are given in table I. The cylinder radii are chosen so that the variation in shearing stress across the annulus for any set is less than 15 percent. The maximum rate of shear is 4000 seconds<sup>-1</sup>. Since the maximum shearing stress is about 250,000 dynes/cm<sup>2</sup>, a maximum Newtonian viscosity of 125 poises can be measured at a rate of shear of 2000 seconds<sup>-1</sup>, and one of 2500 poises at a rate of shear of 100 seconds<sup>-1</sup>. The friction is held small, so that viscosities down to about 0.05 poise can be measured.

The critical Reynolds numbers, at which turbulent flow would start (ref. 11), and the maximum Reynolds numbers for the three cylinder sets are given in table I. The maximum Reynolds numbers are calculated for the maximum applied rotational speed of 1600 rpm, for the minimum measurable viscosity of 0.05 poise, and for a density  $\rho$  of 1 gram per cubic centimeter. The data indicate that the critical Reynolds numbers are 15 to 100 times the maximum Reynolds numbers. Thus, laminar flow is always assured in this viscometer.

The cylinders are designed to keep the end effects negligible. This is accomplished by enlarging the cup diameter appreciably at both ends of the cup neck (fig. 3). In that way the forces outside the length  $L$  of the annulus are made negligible compared with the forces exerted on the bob sides within the annular space. Two splash plates are provided to protect the bearings against contamination by material that otherwise might be thrown against the bearings by centrifugal forces. They are designed to introduce only negligible shearing forces.

### Cup-Rotating Device

Figure 4 is a block diagram of the apparatus. The cup is driven at speeds continuously varying from 0 to 1600 or 0 to 400 rpm, depending on the selected fixed gear ratio between cup and motor.

The drive motor is a two-phase four-pole servo-type motor. The motor is geared to a d-c tachometer. The motor velocity is regulated by changing the amplitude of one phase by d-c tachometer feedback. The tachometer voltage and a reference voltage are converted into an a-c error signal by a Brown converter. The a-c voltage is fed into a high-gain amplifier of standard design (ref. 12, fig. 12-55).

The speeds of the motor and cup, when subjected to varying loads, are regulated within 8 rpm for the high-speed motor setting and within 2 rpm for the low-speed motor setting. The motor speed is continuously increased and decreased by a motor-driven potentiometer, which varies the reference d-c voltage. The acceleration is constant within 1 percent and independent of torque up to the stalling torque of about  $10^6$  dyne-centimeters. The acceleration can be changed, so that the time required to increase the motor speed from zero to any selected maximum speed is 15, 30, 60, 120, or 240 seconds. The maximum speed is selected manually on a second potentiometer. It can be varied from 300 to 1600 or from 75 to 400 rpm, depending on the selected motor gear setting. The speed setting is reproducible within 0.5 percent.

The program sequence is automatically controlled. Two sequences, as shown in figure 5(a) and (b), are provided to give two types of flow curves.

The recorded velocity is accurate within 1 percent of full scale.

#### Torque-Measuring Device

The force transducers are strain-gage assemblies. Three interchangeable transducer units (fig. 2) and a choice of two bridge excitation voltages permit measurements of forces ranging from 5 to 1300 grams. The transducers are attached to the viscometer stand and linked to the bob through a linkage (fig. 3). The friction force due to the linkage and the bob suspension is about 0.5 gram. The output of the transducers is linear with applied torque within 1 percent of full scale. The accuracy of the recorder is also 1 percent of full scale.

For easy replacement, the three transducers are each mounted on a flat plate. The three plates have identical dimensions and fit snugly into an insert provided for them on the viscometer stand. They are spring-mounted to assure that they are placed repeatedly in the exact position with respect to the bob shaft and that they maintain this position during measurement.

The output ranges are chosen to overlap extensively. This is necessary since large ranges of shearing stresses are required for the



measurement of each material, if it is to be measured up to high rates of shear. The total supplied range of shearing stress for each set of cylinders is given in table I.

### Temperature Bath

The constant-temperature bath (fig. 1) is mounted on runners and moves in grooves, so that it can be readily moved in and out for changing samples. Stops provide correct positioning. A thermostat controls the opening and closing of solenoid valves that regulate the flow of hot and cold water into the bath. Temperature control within  $0.2^{\circ}$  C over a range of temperatures from  $10^{\circ}$  to  $50^{\circ}$  is obtained.

### Accessories

High-viscosity materials, such as high polymers and silicones, have the tendency at high rotational speeds to climb out of the annulus. This emptying of the annulus leads to incorrect flow curves, as will be shown later. To avoid such occurrences, a cup guard (figs. 2 and 3) is placed on top of the annulus. The cup guard is designed so that the shearing forces within its confines are negligible compared with those in the annulus.

It is rather difficult to fill the relatively narrow neck of the cup with highly plastic materials, such as printing inks, butter, and petrolatum, without entraining air in the material. The entrainment of air, especially when the air is dispersed, leads to an erroneous flow curve. A piston pump (fig. 2) is provided to assist in filling the cup properly with such materials. Its outside cylinder fits tightly in the upper part of the cup. Thus, material that has been carefully placed in the wide bottom part of the cup can be sucked into the cup neck. If this is done slowly and carefully, air bubbles can be avoided.

### CALIBRATION

The apparent viscosity  $\eta$  of any material is

$$\eta = \tau/G \quad (1)$$

The apparent viscosity of non-Newtonian materials is not a constant, but varies with the applied flow conditions. Therefore, a flow curve - that is, a curve of rate of shear  $G$  against shearing stress  $\tau$  - measured under controlled conditions and over an extended range, is required to evaluate the flow behavior of any non-Newtonian material.

The viscometer produces on the x-y recorder records of rotational speed  $n$  in revolutions per unit time against torque  $T$  under controlled flow conditions. These records represent flow curves if the rotational speeds are directly proportional to rates of shear and the torques proportional to shearing stresses.

The quantities  $G$  and  $\tau$ , however, are not only functions of speed and torque, respectively, but also of the radius. Thus, both  $G$  and  $\tau$  vary somewhat across the annulus, although this rotational viscometer was designed to keep the variations in  $G$  and  $\tau$  small. For flow curves, mean values of  $G$  and  $\tau$  should be plotted. Since the annuli for all three cylinder sets are small, the rate of shear and shearing stress at the midpoint between cup and bob approximate mean values that are used in the calculations.

After integrating the velocity distribution in a concentric-cylinder rotational viscometer (refs. 13 and 14), the midpoint rate of shear  $G$  is

$$G = K_G(2\pi n) \quad (2)$$

where

$$K_G = \frac{8}{(R_b + R_c)^2 \left( \frac{1}{R_b^2} - \frac{1}{R_c^2} \right)}$$

and the midpoint shearing stress  $\tau$  is

$$\tau = K_\tau T \quad (3)$$

where

$$K_\tau = \frac{2}{\pi(R_b + R_c)^2 L}$$

Equation (2) is rigorously correct only for Newtonian materials, where the relation between  $G$  and  $\tau$  is proportional, and

$$G = \frac{1}{\mu} \tau \quad (4)$$

For Bingham plastics, the relation between  $G$  and  $\tau$  is linear, and

$$G = \frac{1}{\mu} (\tau - f) \quad (5)$$

For Bingham materials, equation (2) is correct only after the shearing stress is high enough to initiate shear across the total width of the annulus; that is, if  $\tau \geq f$  at every point in the annulus. The rate of shear at which this happens depends on the flow parameters of the material and on the design parameters of the instrument. In this instrument it is usually small, and equation (2) is essentially valid for most Bingham plastics. This is shown by using the following equation (ref. 15):

$$n \approx \frac{f}{2\pi U} \left[ \frac{R_c^2}{2R_b^2} - \frac{1}{2} - \ln \left( \frac{R_c}{R_b} \right) \right] \quad (6)$$

Since the expression in the brackets of equation (6) is small, ranging from about 0.002 to 0.013 for the three cylinder sets,  $n$  in equation (6) is small even for large ratios  $f/U$ .

The yield value  $f$  is proportional to the torque intercept of the flow curve (ref. 15). That is,

$$f = K_f T_{int} \quad (7)$$

where

$$K_f = \frac{\frac{1}{R_b^2} - \frac{1}{R_c^2}}{4\pi L \ln \left( \frac{R_c}{R_b} \right)}$$

Numerically,  $K_f \approx K_\tau$  (table I) for the three cylinder sets.

For pseudoplastic and dilatant materials where the relation between  $G$  and  $\tau$  is nonlinear, equation (2) is an approximation. Its validity depends on the degree of structural change with rate of shear of these materials and on the design parameters of the instrument. For many such materials, it was found experimentally (ref. 16) that the flow curve fitted an equation of the type

$$G \propto \tau^N \quad (8)$$

where  $N < 1$  for dilatant materials and  $N > 1$  for pseudoplastic materials.

For materials having flow curves that obey equation (8), equation (2) is correct after dividing  $K_G$  by a constant  $C$  (refs. 13 and 17) where

$$C = \left\{ \frac{1 - \left(\frac{R_b}{R_c}\right)^{2N}}{N \left[ 1 - \left(\frac{R_b}{R_c}\right)^2 \right]} \right\} \left( \frac{R_b + R_c}{2R_b} \right)^{2(N-1)} \quad (9)$$

and  $C = 1$  for  $N = 1$  and  $C \rightarrow 1$  for  $R_b/R_c \rightarrow 1$ .

In figure 6,  $C$  is plotted as a function of  $N$  for different ratios of  $R_b/R_c$ . Thus, after  $N$  is obtained from the flow curve,  $C$  can be found from figure 6 or equation (9) for the ratio of  $R_b/R_c$  for the cylinder set used (table I).

For some materials,  $N$  varies with rate of shear, and then the rate of shear  $G$  is no longer a linear function of  $n$ , since  $C$  is now a variable. This introduces an error when correcting equation (2) by dividing  $K_G$  by a constant value of  $C$ . However, even when using equation (2) without any correction, the error is less than 5 percent for materials of  $N \leq 12$ , if cylinder set 1 is used, and for materials of  $N \leq 8$ , if cylinder set 3 is used, since then  $C \leq 1.05$  (fig. 6). Since very few materials exist where  $N > 8$ , equation (2) without correction is accurate within 5 percent for most pseudoplastic materials, provided the proper cylinder set was selected for the measurement. For dilatant materials the error is always less than 5 percent, since  $C$  is never less than 0.95.

Thus, the records of  $n$  against  $T$  measured under controlled conditions do represent flow curves for most materials. The proportionality factors  $K_G$  and  $K_\tau$  are given in table I.

The accuracy of equations (2) and (3) and of the calibration of the tachometer and strain-gage outputs is shown in figure 7. The viscosity of a number of Dow Corning, series 200, silicone fluids was measured by using the three sets of cylinders and all combinations of tachometer and strain-gage outputs. The viscosity of these same oils was also measured at the same temperature ( $25^\circ\text{C}$ ) with Ostwald capillary viscometers of various sizes. Figure 7 is a plot of the ratio of the rotational-viscometer viscosity  $\mu_R$  to the Ostwald-viscometer viscosity  $\mu_0$ , against the Ostwald-viscometer viscosities  $\mu_0$ . The data cover a range of viscosities from about 0.1 to 50 poises. Each point was averaged from as many transducer conditions as was feasible. The data comprise all possible conditions of the instrument. Some of the higher-viscosity oils showed non-Newtonian flow behavior at the higher rates of shear in the rotational viscometer, but the Newtonian initial viscosity at the very low rates of shear was always used in figure 7. This is justified, since the rate of shear in the Ostwald viscometers was always low. Figure 7 indicates that the calculations of  $K_G$  and  $K_\tau$  are good. It also indicates that the end effects are negligible, since end effects, if

present, would have produced a constant positive error of similar magnitude for all three cylinder sets. The maximum error of the rotational-viscometer viscosities, when comparing the values measured with the different cylinder sets, is  $\pm 4$  percent; and the maximum difference, when comparing the rotational- and Ostwald-viscometer viscosities, is  $\pm 5$  percent. This difference is small, considering that both instruments have different inherent errors due to experimental procedure.

#### MEASUREMENTS

Two recorded flow curves of a Newtonian silicone fluid are presented in figure 8. Each line consists of two coinciding records taken at increasing and decreasing rates of shear, called up curves and down curves. The curves were taken with the program switch in position I (fig. 5(a)) with two different pairs of timing gears (fig. 1) for  $\theta = 15$  and 240 seconds, where  $\theta$  is the time of the measurement from zero to the highest applied rate of shear. The lines are straight, have no intercept, and are parallel. This indicates smooth operation, negligible friction, complete reproducibility, and no change with timing  $\theta$ .

Figure 9 is a similar flow curve for a pseudoplastic material of Vistanex in decalin. It was taken with the program switch in position I. First an up and down flow curve was obtained up to a maximum speed of about 1300 rpm. Then, to magnify the lower part of this flow curve, a second flow curve was taken with the motor gears selected to give a maximum speed of about 170 rpm with a correspondingly magnified torque scale. The time per 100 rpm was chosen to be about the same in both curves. Figure 9 demonstrates that the lower parts of a flow curve can be magnified. The reproducibility was good, as can be ascertained by comparing the data.

A suspension of a pigment ( $\text{TiO}_2$ ) in a silicone fluid was used to obtain the flow curves in figure 10. Since this suspension seemed to show thixotropic flow behavior, these curves were taken with the program switch in position II, giving the sequence as shown in figure 5(b). The program switch was set to produce a record of one up curve and two down curves, one having its maximum speed at about 160 and the other at about 320 rpm. The degree of thixotropic behavior of a material can be evaluated (ref. 18) from the flow conditions at two rates of shear. It has been assumed (ref. 18) that a rapidly measured down curve of a thixotropic material yields the flow properties and describes the flow behavior of the material at that point on the up curve at which the down curve is commenced, which is the point of maximum speed of the down curve. Thus, two down curves a and b have to be measured to obtain the flow conditions of the material at two rates of shear or at two up-curve points A and B, respectively. After the first down curve a was measured, the material was left unsheread for 2 minutes to give it a chance to rebuild some of the broken-down structure. [To do that, the program (fig. 5(b)) had

been advanced from 1 over 2 to 3 and was held between 3 and 4.] Then, the cup was accelerated rapidly (in about 1 sec) to a speed of 160 rpm. (The program was continued over 4 to 5.) The up curve was immediately continued, since the torque was less than obtained before at point A. (The program was advanced to 6 as rapidly as possible and continued over 7 to 8.) The torque difference at A is small, and the up curve is almost the same as if it had been recorded without interruption.

Figures 10(a) and (b) differ only in respect to the time taken to measure the up curve. The total up curve in figure 10(a) was measured in 15 seconds; while the one in figure 10(b) was measured in 240 seconds, with resulting smaller loop, lower torque readings on the up and down curves, and lower plastic viscosities, as indicated by the increasing slope of the down curves. Both of the second measurements in figure 10 were made 10 minutes after the respective first ones. The narrow loops and the position of the curves in the second measurements indicate that hardly any build-up of structure occurred during those 10 minutes between measurements. Therefore, temperature increases due to the shearing action could have had only a relatively small effect on the position and areas of the loop.

At the low speeds (see the sections set off by dashed lines in figs. 10(a) and (b)), the torque change was very rapid, probably because of thixotropic breakdown. In fact, the change might have been too rapid for the instrument to follow, especially in the case of figure 10(a), where the acceleration in rate of shear was also high; the time per 100 rpm was less than 5 seconds.

To study the breakdown in thixotropic structure at those low rotational speeds, a suspension similar to that used for figure 10 was prepared, and time-torque curves were measured at different cup speeds of less than 35 rpm. Time-torque curves such as shown in figure 11 are produced by moving the paper at a constant linear speed while the cup is rotated at a constant speed. The torque decreased with time rapidly at first and then more slowly. The two down flow curves shown in figure 12 with a maximum rotational speed of less than 35 rpm were constructed from such time-torque curves. Each two torque values at the same speed were taken from one time-torque curve at the respective times  $t_1$  and  $t_2$ . The two down flow curves are almost parallel and have different intercepts; that is, this material, when subjected to rotational speeds of less than 35 rpm over a period of time, showed a decrease in yield value, while its plastic viscosity remained almost unchanged. Therefore, it can be concluded that the very rapid decrease in torque at the low angular speeds within the areas marked off in figure 10 is mostly caused by thixotropic breakdown in yield value, although thixotropic breakdown in plastic viscosity is most prominent at the higher rotational speeds (fig. 10).

The second measurement in figure 11 was made 2 minutes after the first one, to determine whether temperature increase produced by the shearing action was responsible for the decrease in torque. Only a very small amount of structure did rebuild in those 2 minutes of rest, indicating that a temperature increase would hardly have been responsible for the major part of the decrease in torque.

Figure 13 is included to demonstrate the types of curves that can result when the anomalous behavior of the material or of the instrument upsets the calculated flow pattern. Such curves, when mistakenly considered to be flow curves of the material and used for calculations of flow parameters, lead to errors and misinterpretations.

Many high-viscosity materials, even with the most carefully aligned instrument, gave anomalous curves, similar to measurement 1 in figure 13(a). Such curves can lead to misinterpretations, because the loops can be similar to those obtained from thixotropic materials. The material used in figure 13(a) is a silicone fluid ( $\mu = 350$  poises at  $25^\circ\text{C}$ ). Curves similar to measurement 1 were repeatedly obtained for this fluid. Experiments revealed that such materials when rotated above a certain speed climb out of the annulus. To prevent this, the cup guard (fig. 2) was designed. Measurement 2 in figure 13(a) represents a flow curve obtained under the same conditions as the first curve, but with the cup guard in place. It is a smooth curve, showing only a very small loop area, which indicates that the cup guard served its purpose.

Misalignment of the cup and bob axes can also give curves that lead to misinterpretations, as is demonstrated in figure 13(b). A pseudo-plastic material (Vistanex in decalin) was chosen to demonstrate this point. Both curves in figure 13(b) were taken with the cup guard in place. For the first measurement, the cup axis was purposely misaligned, so that it was not parallel with the bob axis. A loop and oscillations appeared in the recording. Often loops are obtained without such severe oscillations, especially when the misalignment is caused by a bent bob axis. Before the second measurement, the cylinder assembly was realigned by carefully adjusting and straightening both cylinder axes after checking the cup and bob motion and the parallel position of the two axes with the indicator assembly. The resulting second curve is considered to be the flow curve of the material. The up and down curves almost coincide, and the record is smooth.

For the study of certain flow problems, the investigator might like to measure the dynamic flow properties of a material. Figure 14 is included to show that the viscometer can be adapted for dynamic measurements, that is, measurements of the flow properties of a material subjected to sinusoidal oscillations. In this viscometer the cup is oscillated by replacing the reference d-c voltage, which normally controls the cup speed, by the output of a low-frequency oscillator. The dynamic

measurements were made over a frequency range of 0.1 to 4 cycles per second. Reduced frequencies were obtained by adding the circular frequency to the rate of shear at zero frequency. The dynamic and steady-state apparent viscosities, when plotted against reduced frequency and rate of shear, respectively, as in figure 14, should fall on one curve (ref. 19) if the material is a Maxwell liquid. The material used for figure 14 is a solution of Vistanex in kerosene, which gives a pseudo-plastic flow curve. Similar solutions have been shown (ref. 19) to behave like Maxwell liquids.

Lewis Flight Propulsion Laboratory  
National Advisory Committee for Aeronautics  
Cleveland, Ohio, May 5, 1955

## REFERENCES

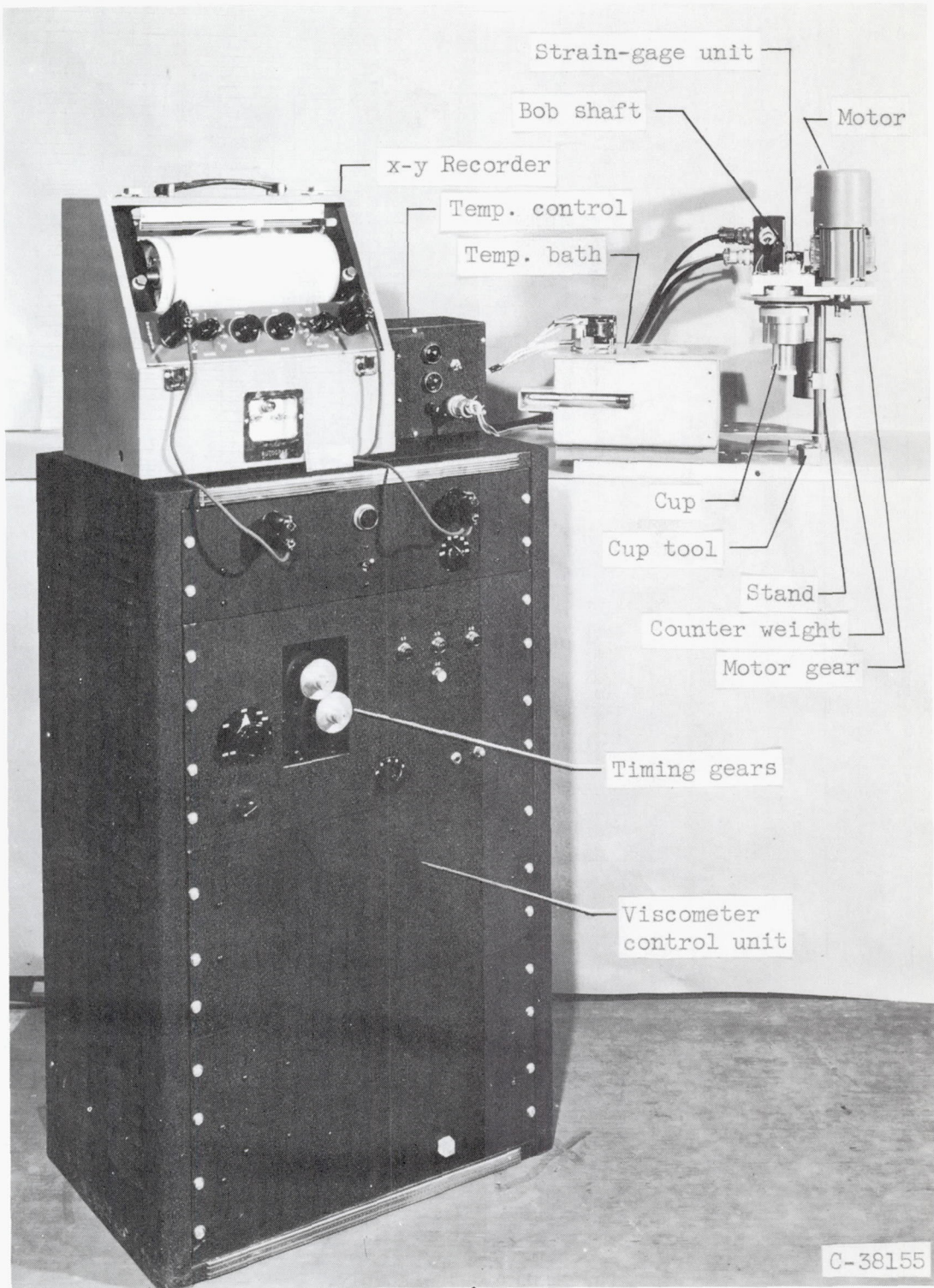
1. Green, Henry: High-Speed Rotational Viscometer of Wide Range. *Ind. and Eng. Chem., Anal. ed.*, vol. 14, July 15, 1942, p. 576.
2. Weltmann, Ruth N.: A Flow-Curve Recorder for a Rotational Viscometer. *Rev. Sci. Instr.*, vol. 16, no. 7, July 1945, pp. 184-191.
3. Buchdahl, R., Curado, J. G., and Braddicks, R., Jr.: A Variable Speed Rotational Viscometer. *Rev. Sci. Instr.*, vol. 18, no. 3, Mar. 1947, pp. 168-172.
4. Smith, J. Wilson, and Applegate, Paul D.: The Hercules High-Shear Viscometer. *Trade Jour.*, vol. 126, no. 23, June 3, 1948, pp. 60-66.
5. Williams, P. S.: Some Effects on the Flow of Concentrated Suspensions of Variations in Particle Size and Shape. *Discussion Faraday Soc.*, no. 11, 1951, pp. 47-55.
6. Helmes, Erich: Ein registrierendes Viscosimeter zur Aufnahme von Fliesskurven. *Chem.-Ing.-Tech.*, Nr. 7, 1953, pp. 390-394.
7. Pearce, C. A. R.: An Electromagnetic Torquemeter for Use in Viscometry. *Jour. Sci. Instr.*, vol. 30, July 1953, pp. 232-236.
8. McKennell, R.: A Versatile Cone and Plate Viscometer with Automatic Flow Curve Recording. *Proc. Second Int. Cong. on Rheology*, V.G.W. Harrison, ed., Butterworths Sci. Pub. (London), 1954, pp. 350-358; discussion, pp. 358-359.
9. Merrill, Edward W.: A Coaxial Cylinder Viscometer for the Study of Fluids under High Velocity Gradients. *Jour. Colloid Sci.*, vol. 9, no. 1, Feb. 1954, pp. 7-19.



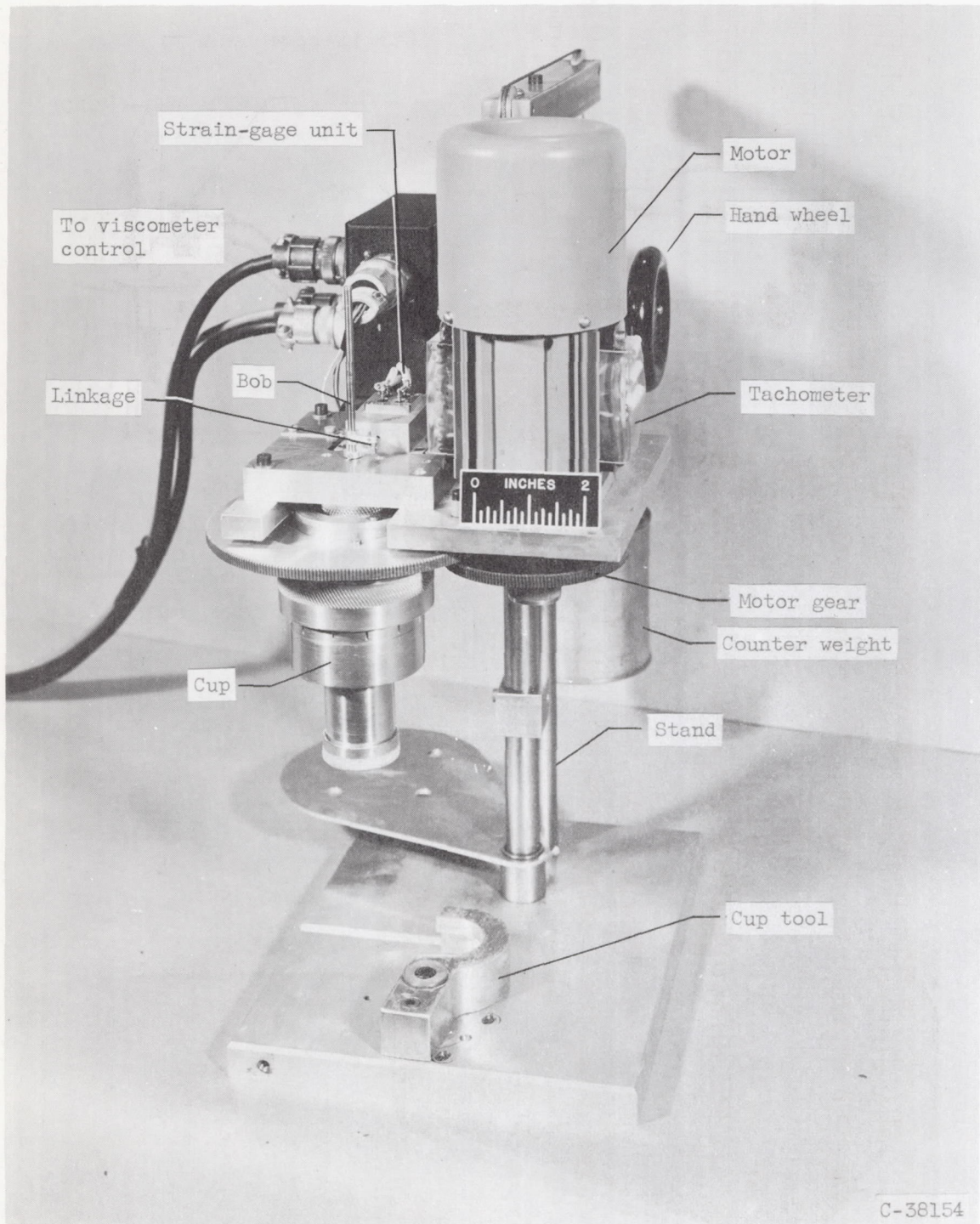
10. Weltmann, Ruth N., and Kuhns, Perry W.: Effect of Shear Temperature on Viscosity in a Rotational Viscometer Measurement. *Jour. Colloid Sci.*, vol. 7, no. 3, June 1952, pp. 218-225.
11. Taylor, G. I.: Fluid Friction Between Rotating Cylinders. *Proc. Roy. Soc. (London)*, ser. A, vol. 157, Dec. 2, 1936, pp. 546-578.
12. Greenwood, Ivan A., Jr., Holdam, J. Vance, Jr., and MacRae, Duncan, Jr., eds.: *Electronic Instruments*. McGraw-Hill Book Co., Inc., 1948, p. 439.
13. Reiner, Markus: *Deformation and Flow - An Elementary Introduction to Theoretical Rheology*. H. K. Lewis and Co. (London), 1949.
14. Reiner, M., and Rivlin, R.: The Theory of Streaming of an Elastic Liquid in a Couette Apparatus. *Kolloid Zs.*, vol. 43, 1927, pp. 1-5.
15. Green, Henry: *Industrial Rheology and Rheological Structures*. John Wiley & Sons, Inc., 1949.
16. Farrow, F. D., Lowe, G. M., and Neale, S. M.: Flow of Starch Paste at High and Low Rates of Shear. *Jour. Textile Inst.*, vol. 19, 1928, pp. T18-T31.
17. Weltmann, Ruth N.: An Evaluation of Non-Newtonian Flow in Pipe Lines. NACA TN 3397, 1955.
18. Green, Henry, and Weltmann, Ruth N.: Thixotropy. Vol. VI of *Colloid Chem.*, ch. 15, Jerome Alexander, ed., Reinhold Pub. Corp., 1946, pp. 328-347.
19. Padden, F. J., and DeWitt, T. W.: Some Rheological Properties of Concentrated Polyisobutylene Solutions. *Jour. Appl. Phys.*, vol. 25, no. 9, Sept. 1954, pp. 1086-1091.

TABLE I. - DIMENSIONS, REYNOLDS NUMBERS, AND SHEARING-STRESS LIMITS OF THREE CYLINDER SETS

Cylinder set	$R_c$ , cm	$R_b$ , cm	L, cm	$K_G$	$K_\tau$ , cm <sup>-3</sup>	$R_b/R_c$	$\tau$ /in. deflection ( $\tau$ in dynes/cm <sup>2</sup> )		$Re = 2\pi n R_c^2 [1-(R_b/R_c)] \rho/\mu$	
									$Re_{cr}$	$Re_{max}$
							Min.	Max.		
1	0.952	0.914	4.305	24.5	0.043	0.96	70	13,800	2,000	122
2	1.026	.914	4.305	9.6	.041	.90	65	12,900	10,000	345
3	.400	.3683	4.326	12.1	.248	.925	408	81,000	5,000	42



(a) Complete assembly.  
Figure 1. - NACA viscometer.



(b) Mechanical assembly.

Figure 1. - Concluded. NACA viscometer.

CB-3 back

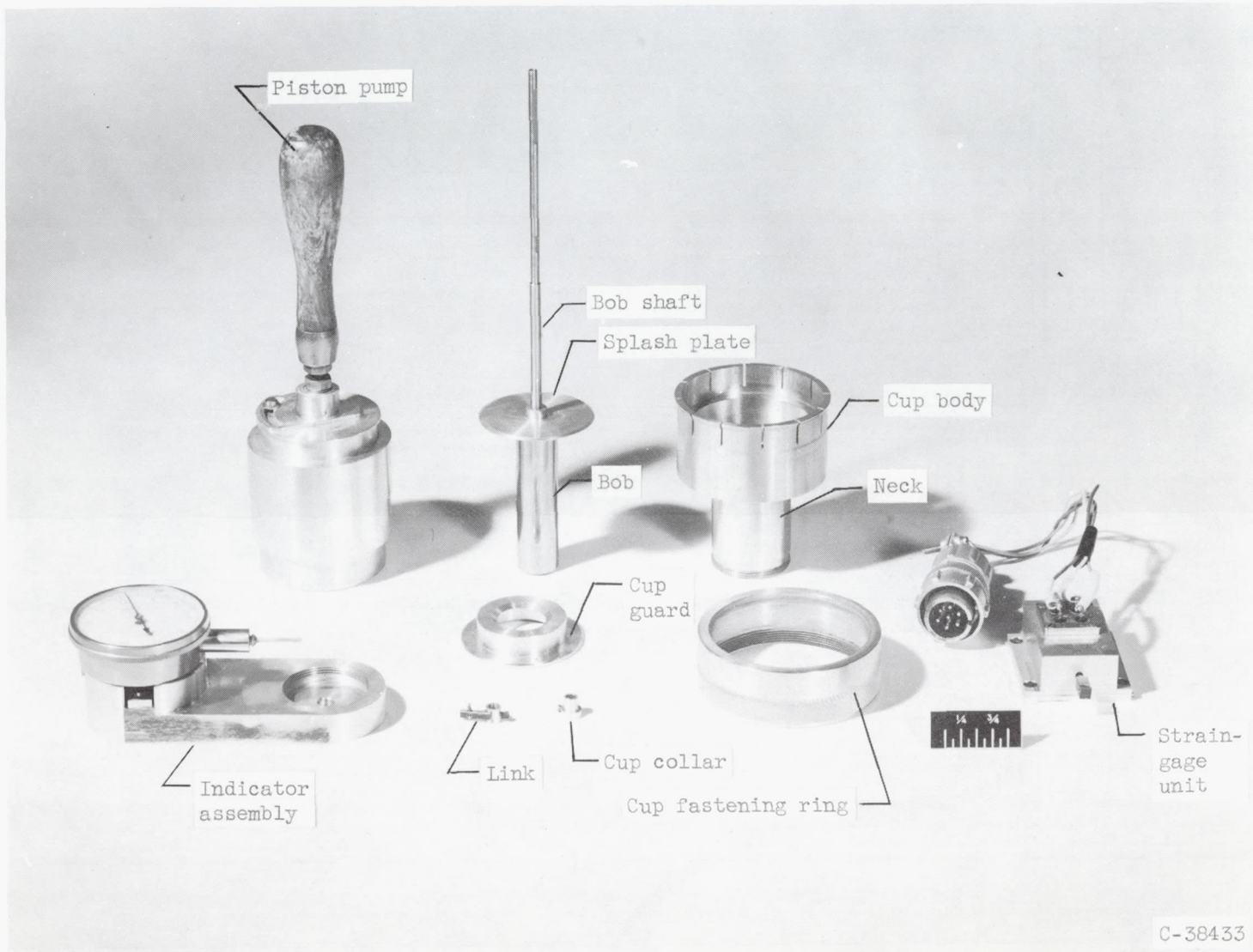


Figure 2. - Viscometer parts.

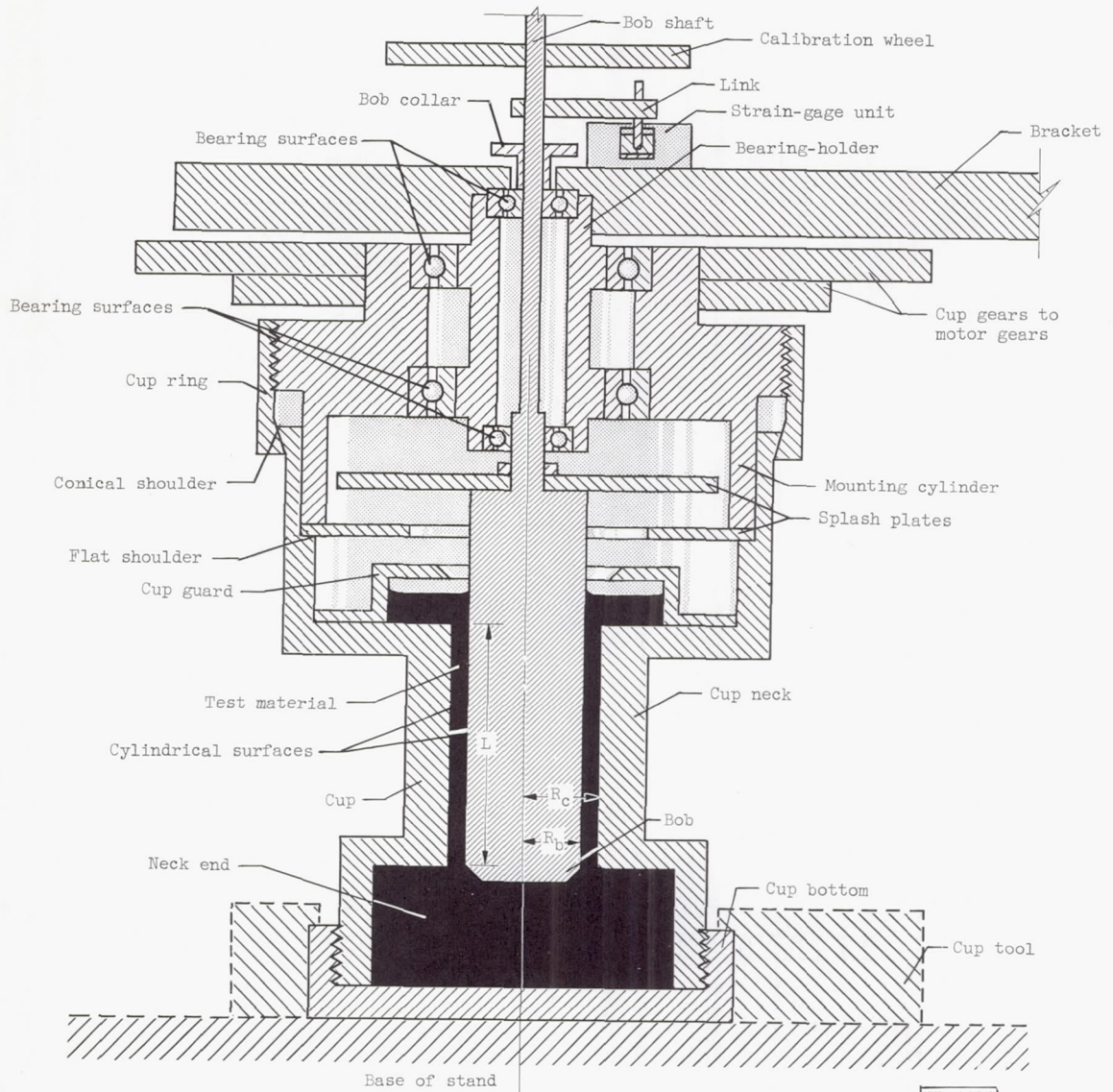
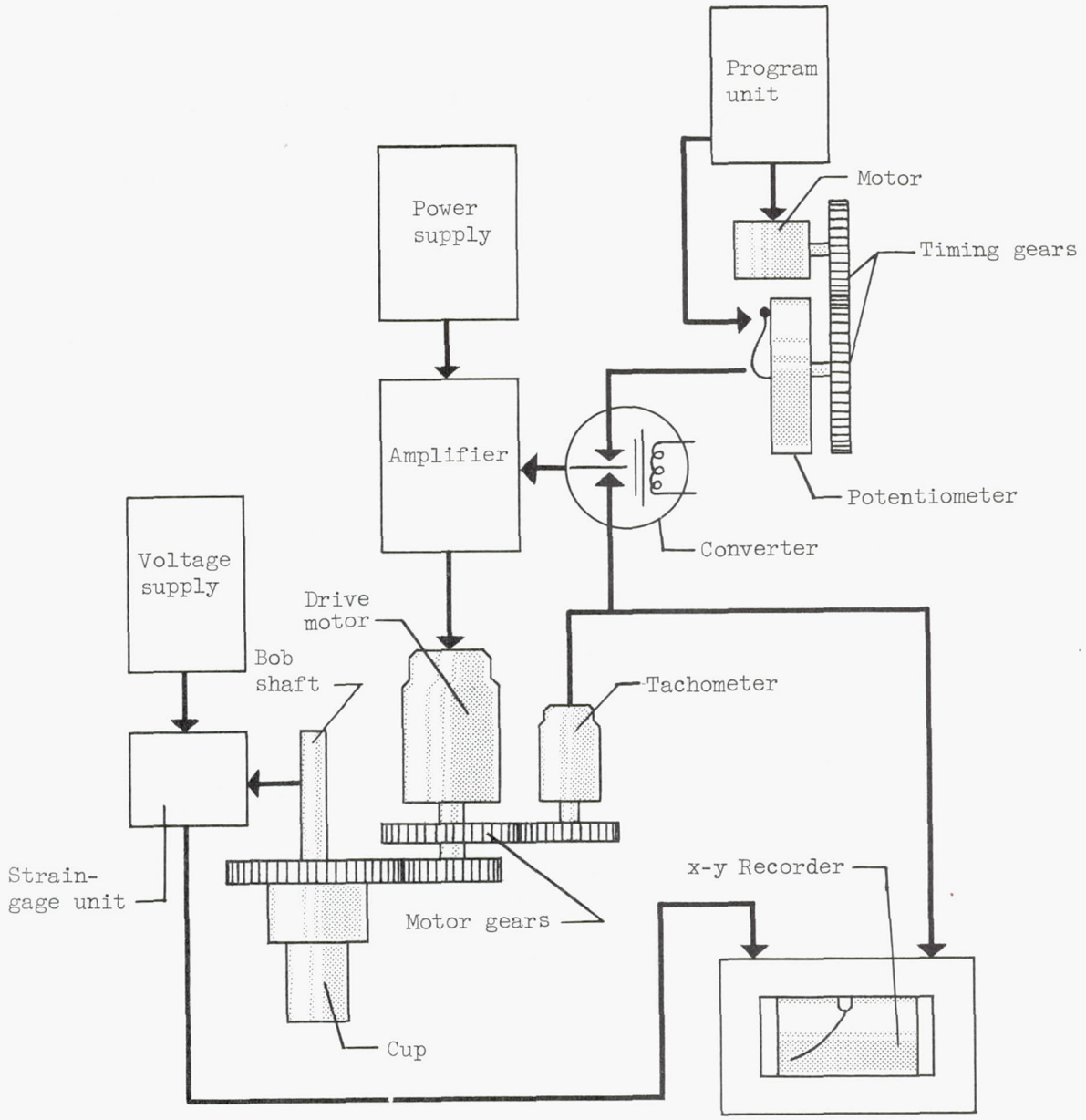


Figure 3. - Diagram of cylinder assembly.

CD-4414

3698



CD-4415

Figure 4. - Block diagram of NACA viscometer.

3698

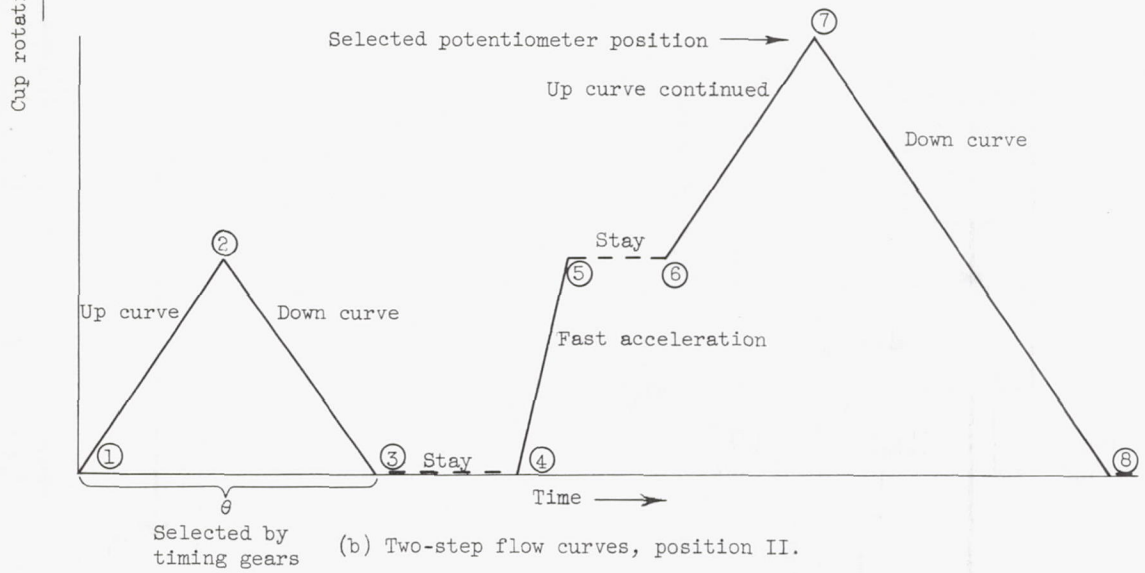
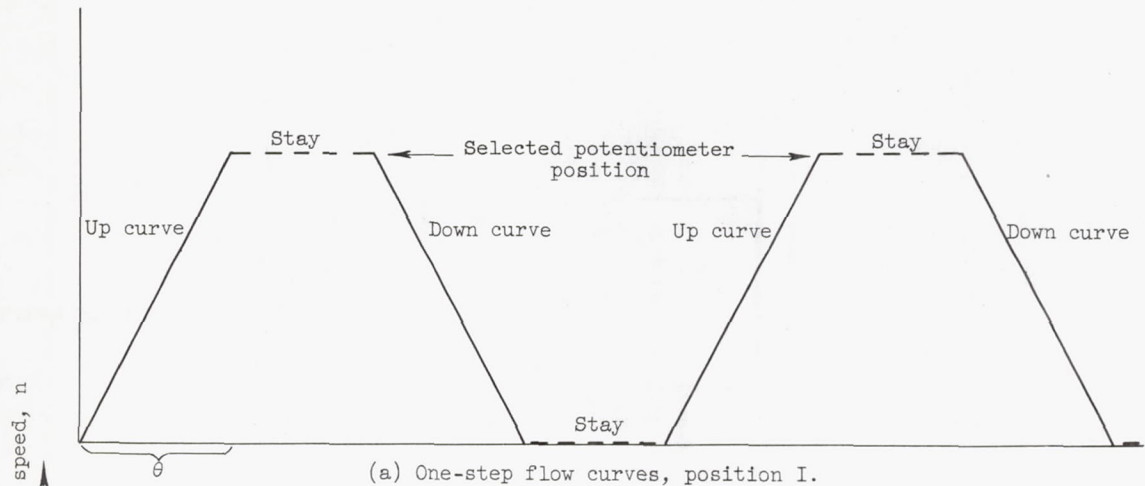


Figure 5. - Program sequences.



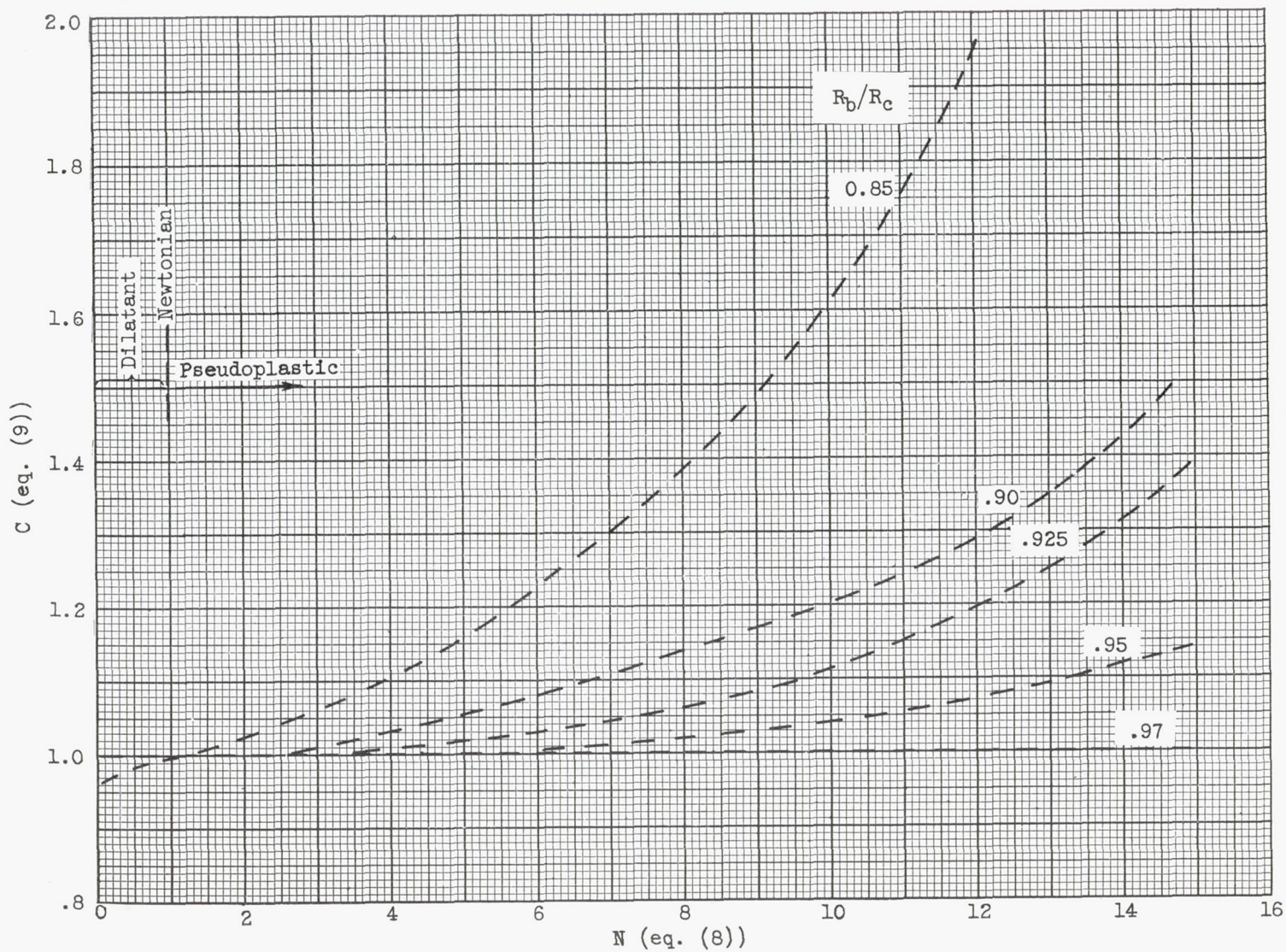


Figure 6. - Rate-of-shear correction for pseudoplastic and dilatant materials (eq. (9)) measured in rotational viscometers.

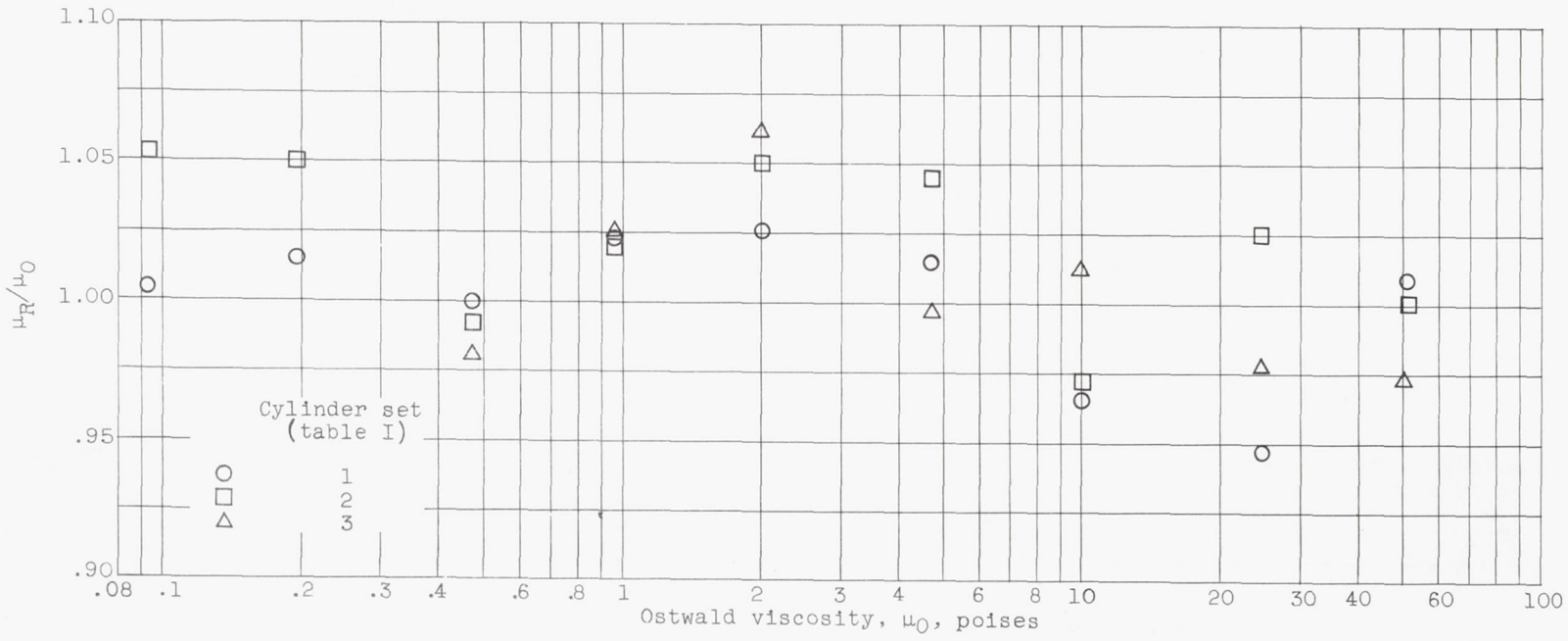


Figure 7. - Calibration check.

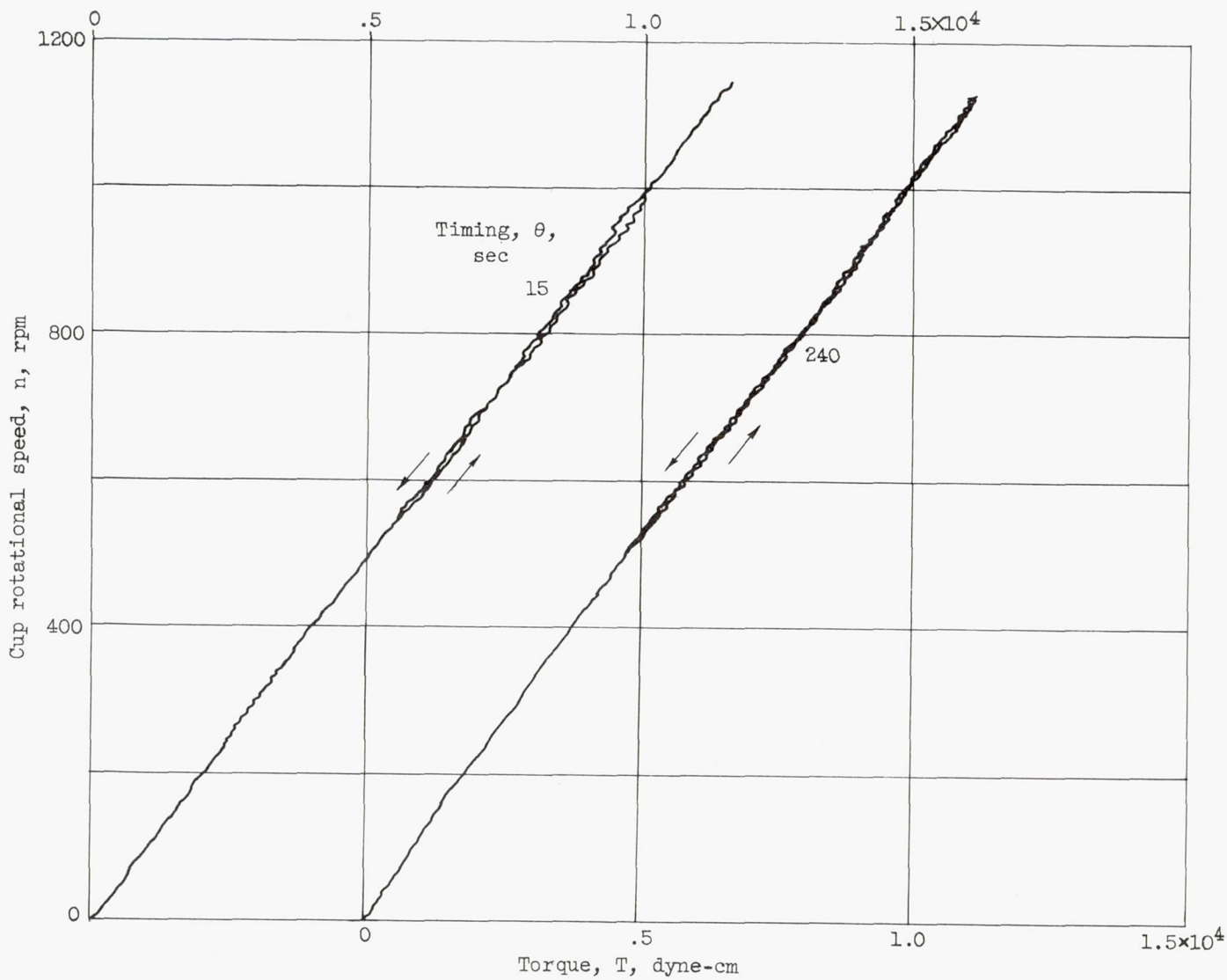


Figure 8. - Flow curves of silicone fluid. Cylinder set 3.

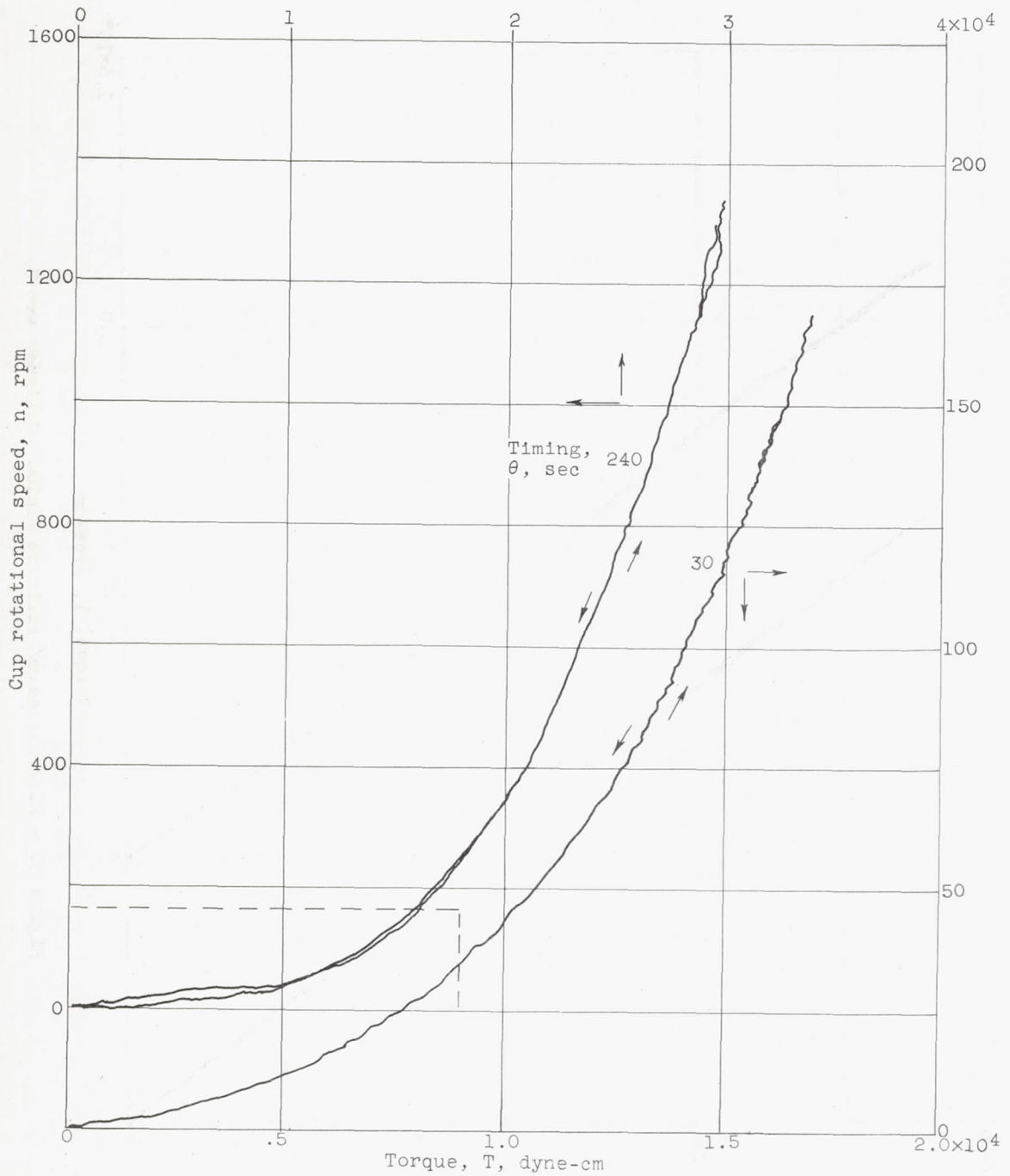
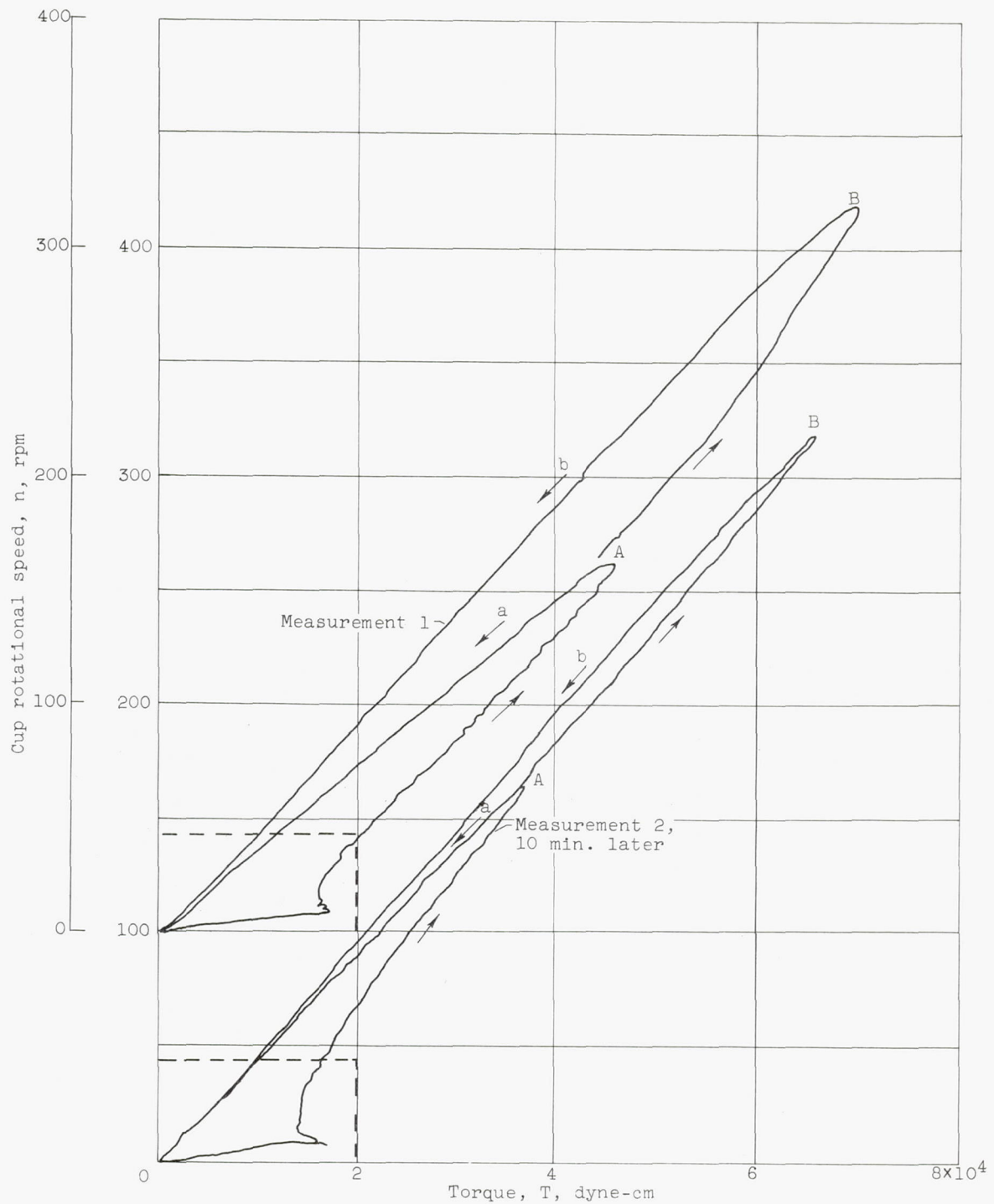
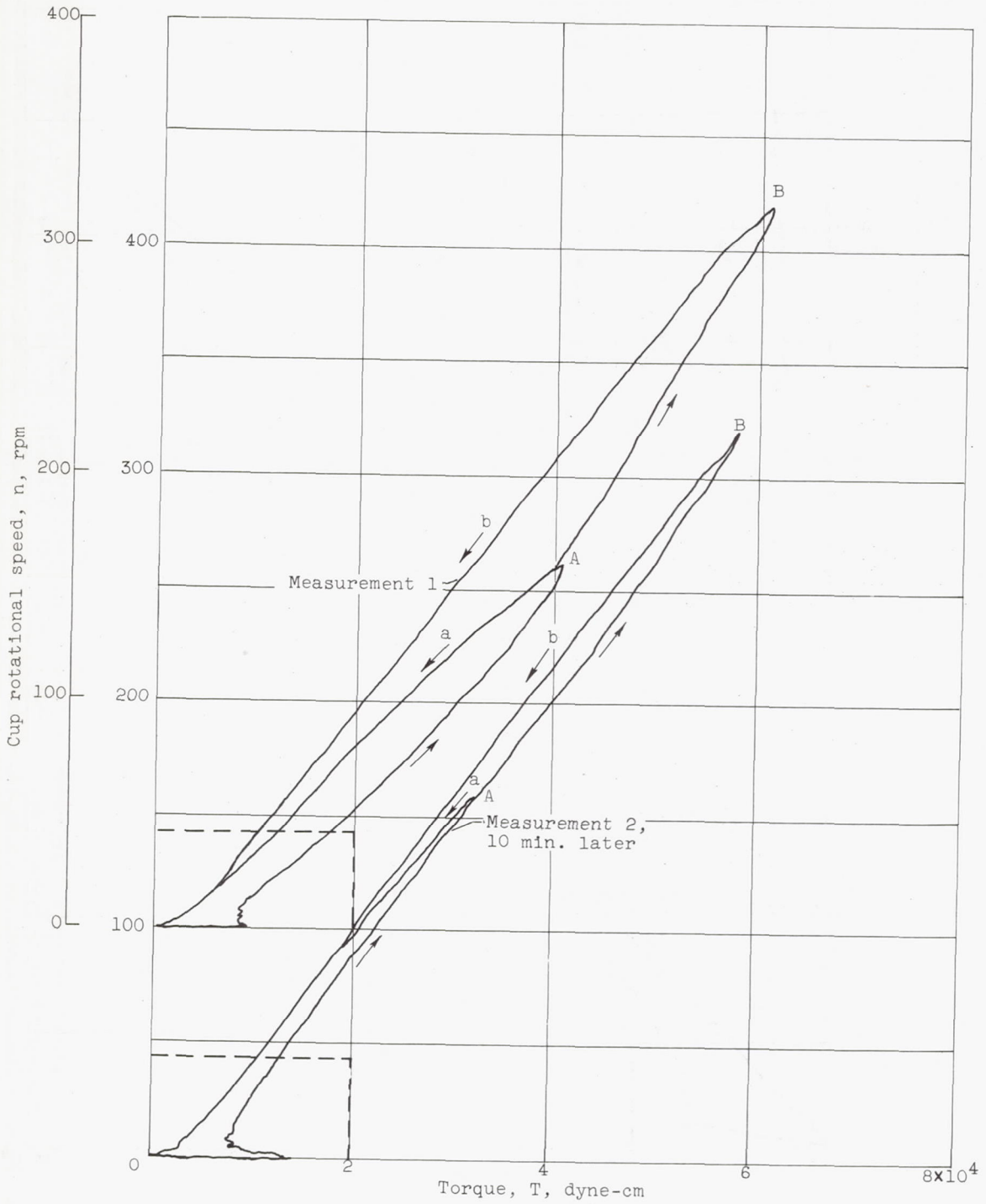


Figure 9. - Flow curves of Vistanex in decalin. Cylinder set 3.  
Time per 100 rpm ~ 17.7 seconds.



(a) Timing  $\theta = 15$  seconds.

Figure 10. - Flow curves of pigment (TiO<sub>2</sub>) in silicone fluid. Cylinder set 2.



(b) Timing  $\theta = 240$  seconds.

Figure 10. - Concluded. Flow curves of pigment ( $TiO_2$ ) in silicone fluid. Cylinder set 2.

3698

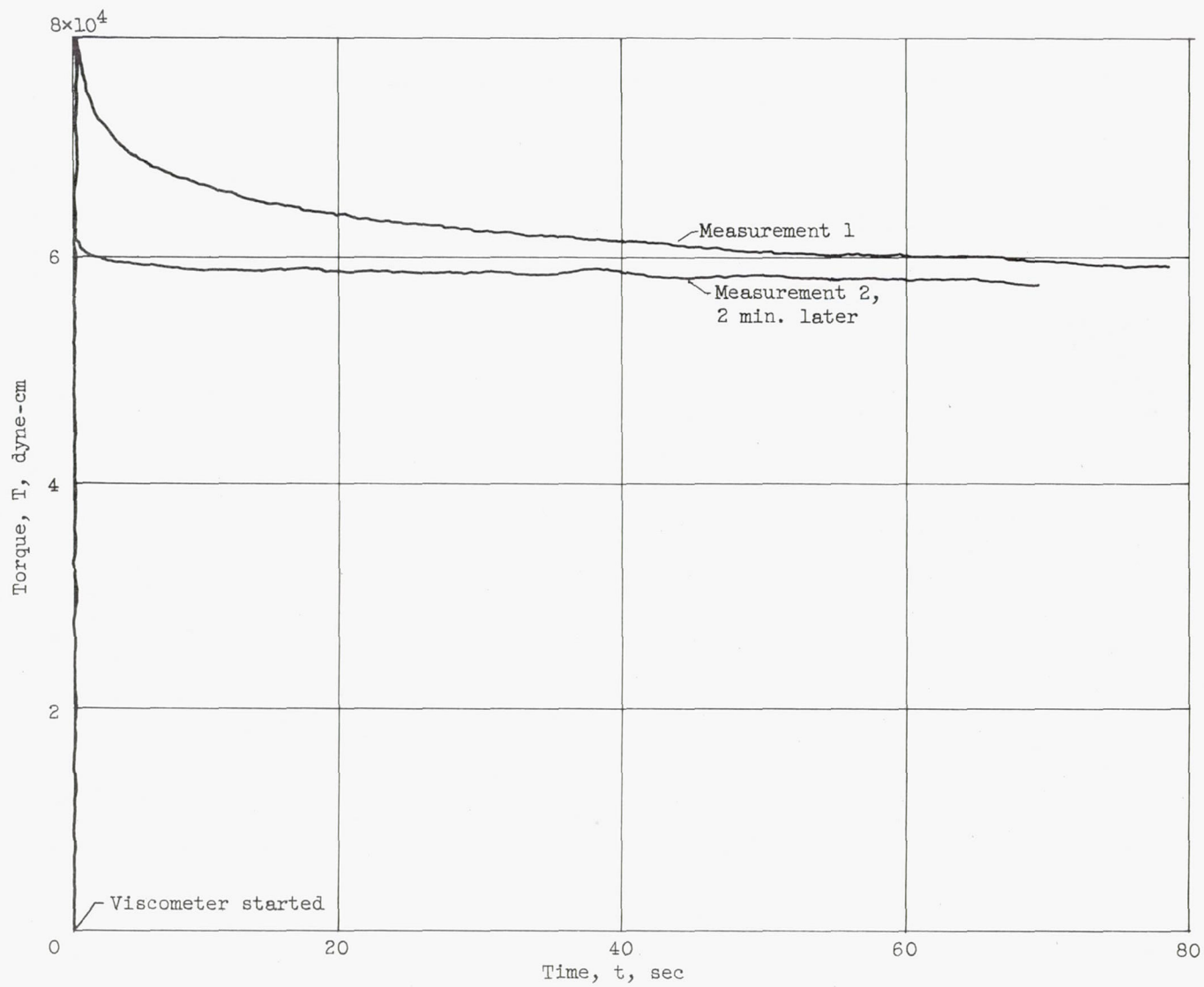


Figure 11. - Torque-time curves of pigment ( $\text{TiO}_2$ ) in silicone fluid. Cylinder set 2; cup rotational speed, 320 rpm.

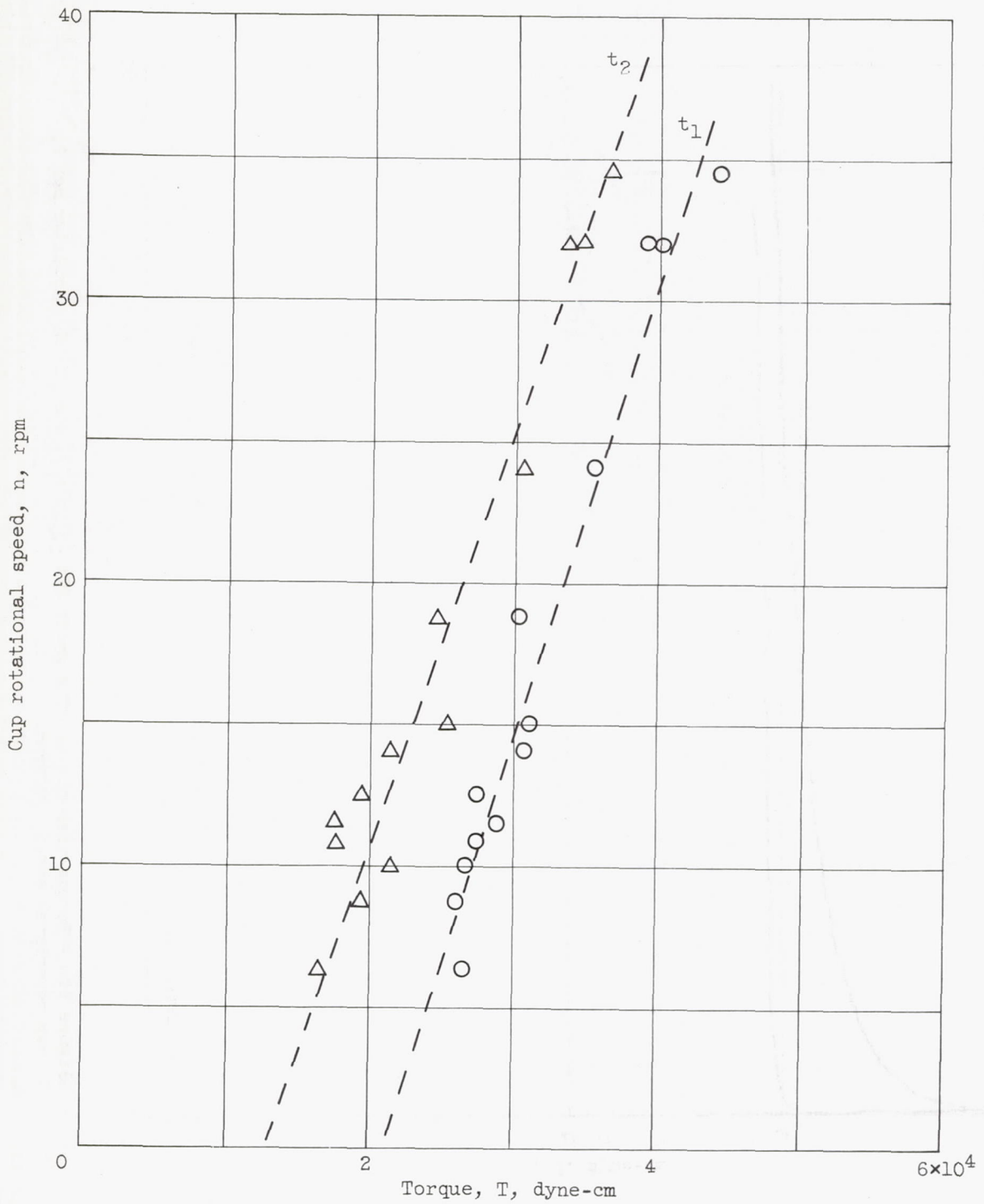
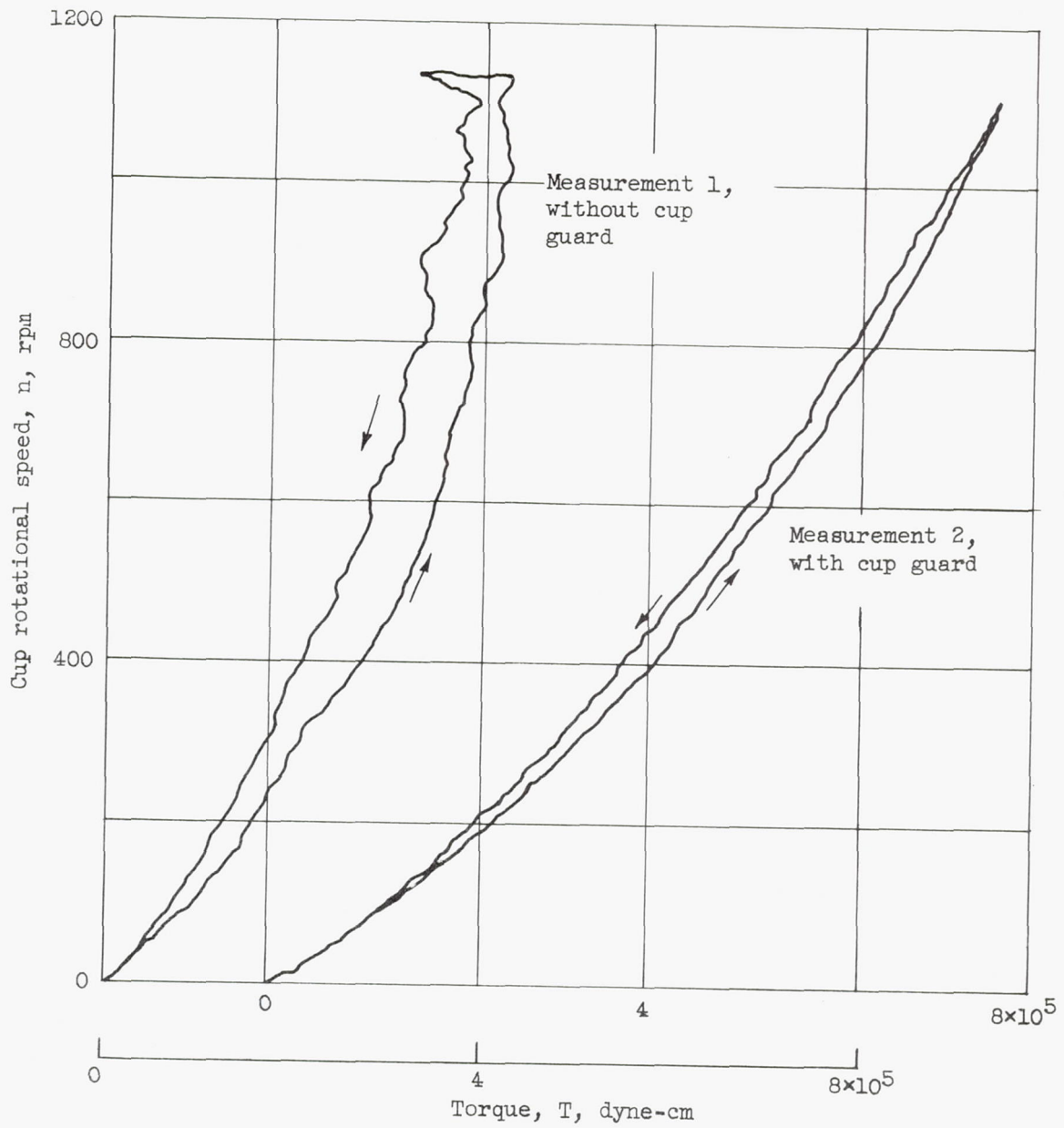


Figure 12. - Down flow curves of pigment ( $TiO_2$ ) in silicone fluid. Cylinder set 2;  $t_2 > t_1$ .

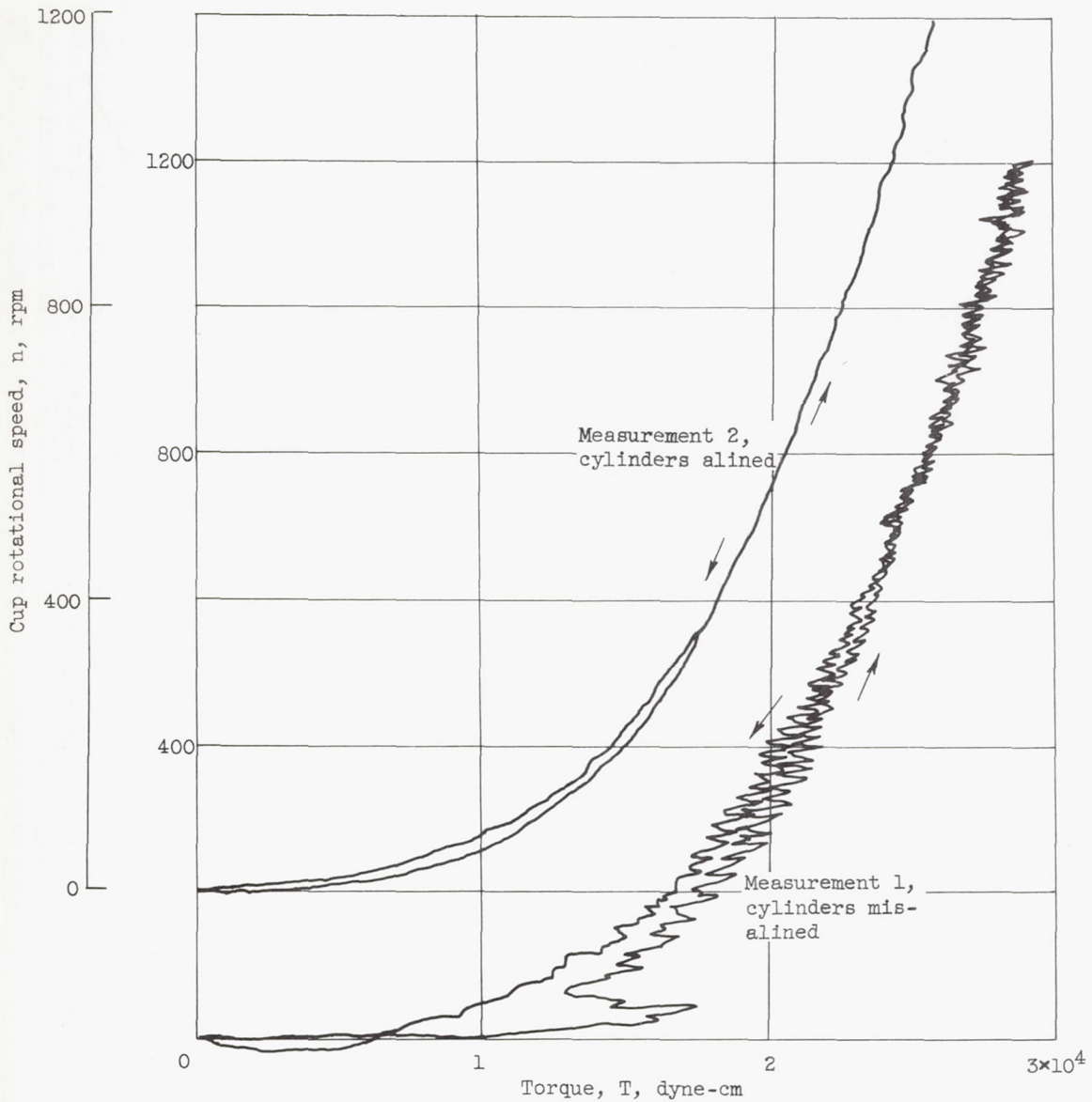
3698





(a) Anomaly due to material leaving annulus. Silicone fluid; timing  $\theta = 15$  seconds.

Figure 13. - Anomalous flow curves. Cylinder set 3.



(b) Anomaly due to misalignment of cylinder. Vistanex in decalin; timing  $\theta = 30$  seconds.

Figure 13. - Concluded. Anomalous flow curves. Cylinder set 3.

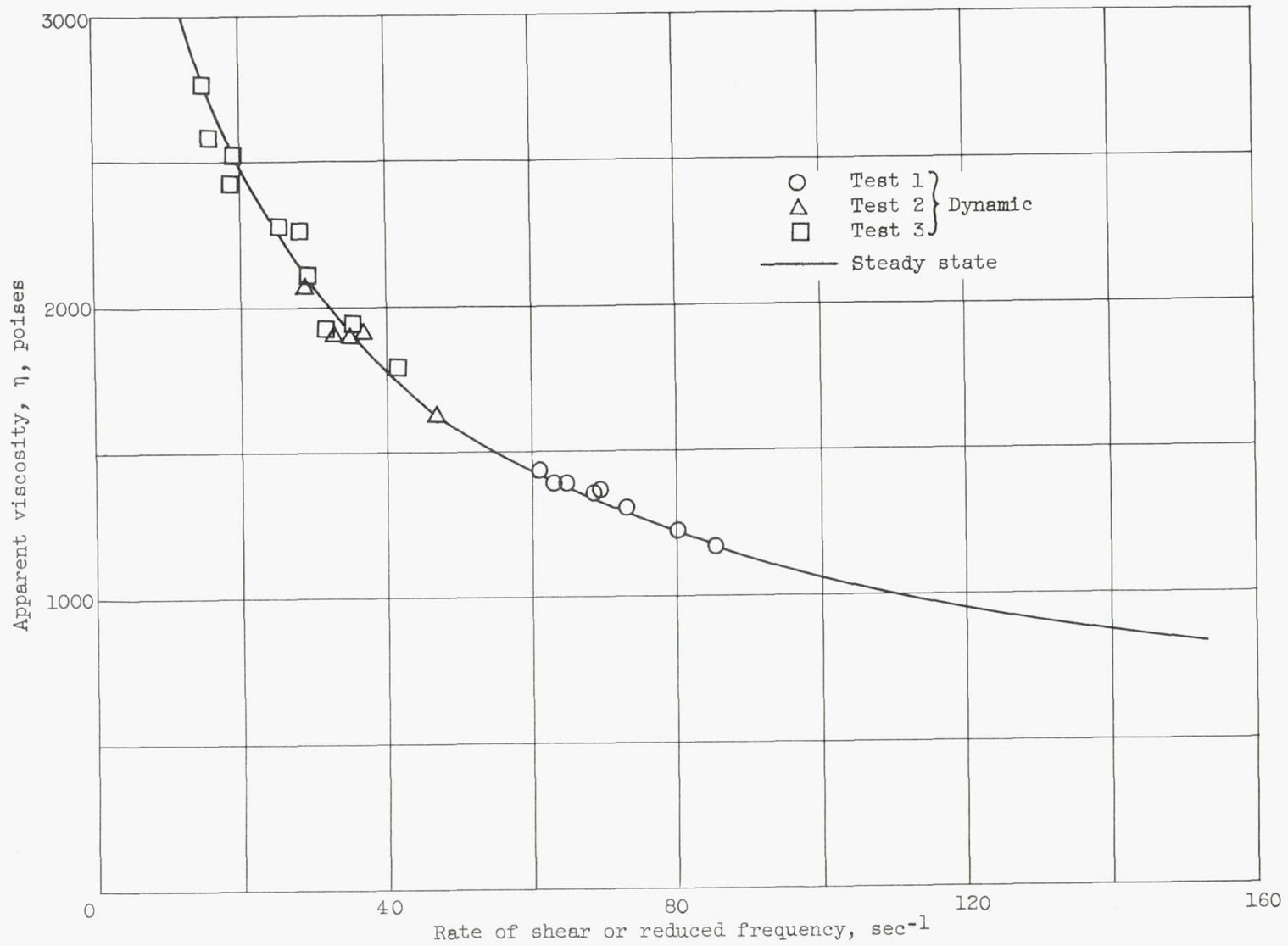


Figure 14. - Dynamic and steady-state flow viscosities of Vistanex in kerosene.